

Cold joining to fabricate large size metallic glasses by the ultrasonic vibrations



Xin Li, Xiong Liang, Zhenxuan Zhang, Jiang Ma*, Jun Shen

Guangdong Provincial Key Laboratory of Micro/Nano Optomechatronics Engineering, College of Mechatronics and Control Engineering, Shenzhen University, Shenzhen 518060, PR China

ARTICLE INFO

Article history:

Received 31 December 2019

Revised 24 March 2020

Accepted 25 March 2020

Keywords:

Bulk metallic glass

Ultrasonic welding

Hardness

XRD

Computed tomography

ABSTRACT

Breakthrough of glass forming ability limitation has been a longstanding pursuit in metallic glasses. In present work, an ultrasonic welding technology was used to achieve this goal. The $\text{La}_{55}\text{Al}_{25}\text{Ni}_5\text{Cu}_{10}\text{Co}_5$ rods were bonded together. Results of computed tomography and scanning electron microscope show that the weld seam tends to narrow gradually and disappear with the increase of welding energy. X-ray diffraction indicated that it preserves completely amorphous structure. In addition, the hardness of the weld position increased with the increase of energy, showing the interfaces bonded together.

© 2020 Acta Materialia Inc. Published by Elsevier Ltd. All rights reserved.

Since the first discovery of metallic glasses in 1960 [1], this kind of material has aroused great attention to many materials researchers. Compared with traditional crystalline alloys, the amorphous structure of metallic glasses endows them with distinctive performance characteristics. Metallic glass ribbons, wires as well as powders have been thought to be potential in industrial fields [2–3]. Bulk metallic glasses (BMGs) also have superior properties such as high strength [4–5], toughness [6], hardness [7], wear resistance [8], corrosion resistance [9–10], catalytic activity [11], soft magnetic properties [12], hard magnetic properties [13], superplasticity [14] et al., and thus have broader industrial application prospects [15]. However, due to metallic glasses need rapid cooling to maintain its amorphous structure in the fabrication process, therefore, the glass forming ability (GFA) has been a longstanding issue and the manufacture of large-sized products and complex-shaped parts has become a major problem for their practical applications [16].

At present, the bulk metallic glasses are mostly produced by the conventional water-cooled copper mold casting, which is a rapid cooling of metallic liquid under argon protection. This means that each metallic glass former has its critical dimension, and the obtained sample size will be fixed. To surmount the GFA restriction that fundamentally limited the application of BMGs, various methods have been developed to enlarge their sizes [17]. Hence, the

welding technology has entered the vision of researchers, which can connect the fabricated metallic glasses together [18]. Generally, the welding of metallic glasses can be divided into two categories. Among them, laser welding [19], electron beam welding [20] spark welding [21] and resistance spot welding [22], even other measures use rapid, local heating like reactive foils to weld [23] are classified as liquid phase welding. In particular, liquid phase welding requires a stable heat source to melt the material for a stable joint, which inevitably heated above the melting temperature (T_m) [24]. And for BMGs, liquid phase joining requires sufficiently-high heating and cooling rates to avoid the crystallization, therefore, the process is complex and the manufacturing costs is rather high. On the other hand, supercooled liquid phase welding of metallic glasses has also been included in research plans by researchers for its lower costs and simple process. So far, supercooled liquid phase connections such as explosive welding [25], ultrasonic welding [26] and friction welding [27] have been proved by scholars to be used for the bonding of metallic glasses, and the joints have relatively good results in terms of welding strength [28]. The supercooled liquid phase welding controls the metallic glasses in the range of the crystallization temperature (T_x) and the glass transition temperature (T_g), i.e., its supercooled liquid phase ΔT_x ($\Delta T_x = T_x - T_g$), to form the joint by its superplasticity.

In these connection methods, the ultrasonic welding process can be used to weld traditional thin layers of metal at low temperature, low pressure, and low energy consumption [29]. Ultrasonic welding can be used to obtain a workpiece with a specified shape [30]. As a promising method, the ultrasonic welding

* Corresponding author.

E-mail address: majiang@szu.edu.cn (J. Ma).

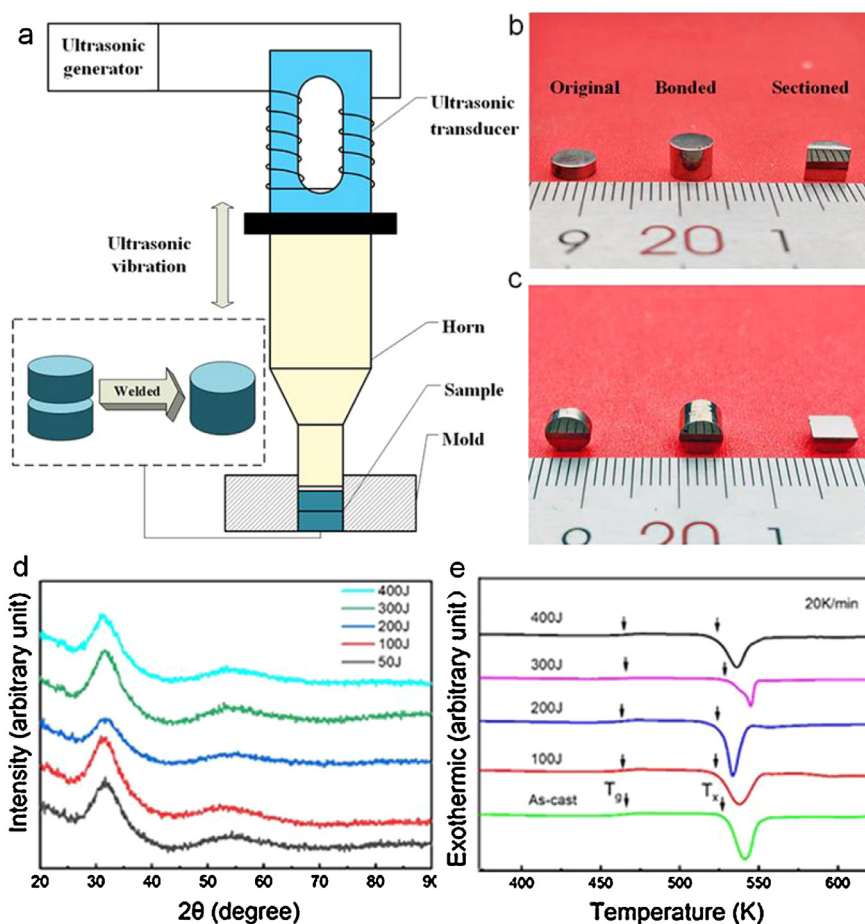


Fig. 1. (a) Ultrasonic welding process sketch: ultrasonic vibration is transmitted from the ultrasonic generator to the horn, and the horn exerts pressure and vibration on the sample to weld it into a whole. (b) (c) The front and vertical views of original sample, bonded sample and sectioned sample. (d) XRD diagram of welding section of La-BMG welding samples with welding energy of 50 J, 100 J, 200 J, 300 J, 400 J and (e) DSC curves of the La-BMG samples with welding energy of 100 J, 200 J, 300 J, 400 J and as-cast metallic glasses.

has been used to join BMGs together to make a larger one, but there are still some problems. Just like the steel strip with smaller welding size [25,31], or the crystallization after welding [32], or the need for external heating and using fillers [33], which will hinder the ultrasonic welding of metallic glass from being widely used. Therefore, an ultrasonic welding method which can obtain complete amorphous structure without filler at room temperature is urgently needed, which could be a salvation of BMGs from the barricades of GFA. In this study, the $\text{La}_{55}\text{Al}_{25}\text{Ni}_5\text{Cu}_{10}\text{Co}_5$ (at.%) metallic glass rods with diameter of 5 mm were used. Through adjusting the welding parameters, metallic glasses were fused to each other into a larger one without crystallization by ultrasonic vibration at room temperature. X-ray diffraction and differential scanning calorimeter are used to verify that the obtained joint is still amorphous, and computed tomography and micro hardness tests are used to ensure welding reliability. Our results may throw lights on accelerating the progress of BMGs in their extensive applications.

An ultrasonic vibration device was used to bond metallic glasses with 20 kHz vibration frequency and maximum power 2500 W, equipment sketch has been shown in Fig. 1(a). Ultrasonic welding was used to bond the $\text{La}_{55}\text{Al}_{25}\text{Ni}_5\text{Cu}_{10}\text{Co}_5$ metallic glasses rods with thicknesses of 2 mm. First, the metals in desired atomic ratio were melted by electric arc as a master alloy and dropped cast into a 5 mm diameter amorphous rod using a copper mold in a Ti-gettered argon atmosphere. Then, this rod was

cut into $\Phi 5 \times 2$ mm blocks by using the low speed diamond cutting machine, and the surface of those blocks to be bonded were sanded with 1000 mesh sandpapers. The left sample in Fig. 1(b) and (c) shows the original sample in front view and top view, respectively. The amorphous structure of the sample was confirmed by x-ray diffraction (XRD, Rigaku- MiniFlex600) analysis at 4θ /min with $\text{Cu-K}\alpha$ radiation. Then, those samples were degreased in an ultrasonic alcohol bath before bonding.

In this experiment, two La-based amorphous alloy samples were placed in the mold cavity, then those samples were fixed in mold and customized horn exerted pressure and ultrasonic vibration to them. Fixed ultrasonic vibration frequency (20 kHz) and welding force (69 kPa), and adjustable ultrasonic energies, and other fixed parameters were used in the bonding process to compare the welding reliability of samples obtained at different energies. A computed tomography (CT, Sanying precision instruments-nano Voxel 3000d) device was used to perform three-dimensional visual characterization of the welded sample. The characteristics and dimensions of the internal defects of the sample will be clearly and accurately displayed. After CT testing, samples will be vertical cut to the weld interface using a low speed diamond cutter, and the section will be simply polished for subsequent characterization as shown in Fig. 1(b) and (c). The amorphous state of La-based welded samples detected by XRD and differential scanning calorimetry (DSC; Perkin-Elmer DSC-8000) with a heating rate at 20 K/min. The microstructures of sample were observed by scan-

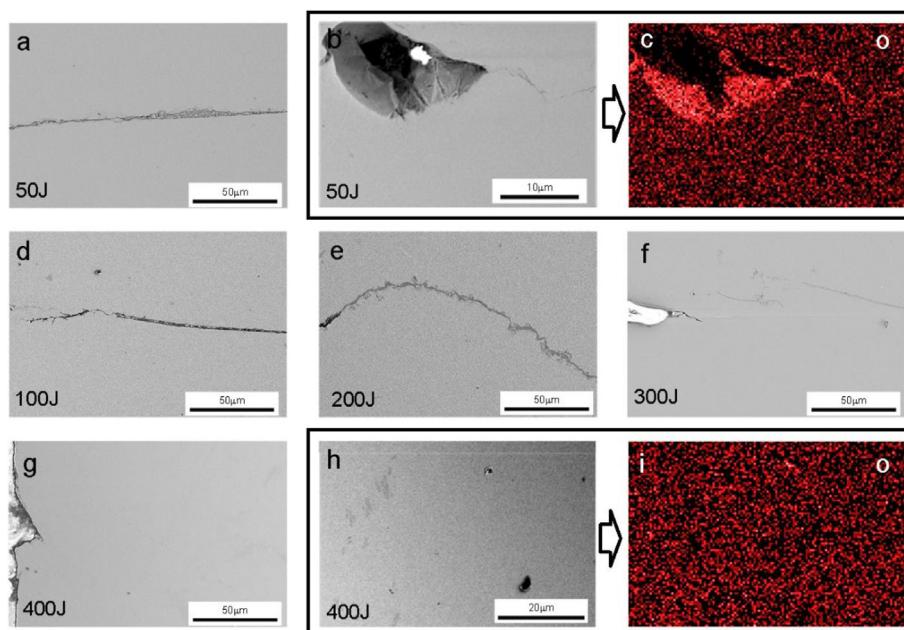


Fig. 2. Cross-sectional SEM micrographs of metallic glasses after ultrasonic welding with energy at 50 J (a), 100 J (d), 200 J (e), 300 J (f), 400 J (g) and oxygen element distribution maps of 50 J (b, c) and 400 J (h, i).

ning electron microscope (SEM, FEI Scios) and the distribution diagram of an element of cutting section was measured by energy dispersive spectrometer (EDS, equipped in SEM). Finally, the surface hardness of the cross section was measured by an automatic Vickers hardness tester at the load of 500 gf (4.90 N) and hold for 10 s, and the hardness of 30 dots perpendicular to the weld line was obtained.

The XRD spectrum in Fig. 1(d) shows the interfacial reaction layer in La-BMG welding joints under different welding energy: 50 J, 100 J, 200 J, 300 J and 400 J. Each curve indicates only a broad halo diffraction peak in the range of 25–40°, which is typically feature of an amorphous structure. It can be judged that the samples obtained under different welding energies have remained completely amorphous joint under ultrasonic vibration. To further confirm that the joint of $\text{La}_{55}\text{Al}_{25}\text{Ni}_5\text{Cu}_{10}\text{Co}_5$ BMG does not contain any Crystallization, a comparison of the DSC traces of different welding energies with 20 K/min was carried out in Fig. 1(e). The thermograms show the typical characteristics of distinct glass transition of metallic glasses. In DSC curve of as-cast sample, the glasses transition temperature T_g was 462 K, and the crystallization point T_x was 528 K. And in the thermograms of welded sample, there is a relatively obvious glass transition phenomenon and a relatively wide supercooled liquid region ($\Delta T_x = T_x - T_g \approx 66$ K) are essentially the same as cast. To have a more careful verification [34], we calculated the enthalpy during the crystallization process in DSC measurement. The enthalpy values are 46.36 J/g (as-cast), 40.74 J/g (welding energy=100 J), 38.29 J/g (welding energy=200 J), 41.23 J/g (welding energy=300 J) and 42.13 J/g (welding energy=400 J), respectively. As for the well bonded samples of welding energies 300 J and 400 J, they show comparable values with the as-cast one. However, when the welding energy is low, the values are a little lower than the cast one. At a low welding energy such as 200 J, the BMG plates cannot form a solid bonding with each other, the friction between them could happen during the ultrasonic hammering, therefore, the temperature may rises higher than the high welding energy samples, resulting in the local slight crystallization.

The cross-sectional SEM micrographs in Fig. 2 shows the joining interfaces produced under different welding energy. As the energy

of ultrasonic welding increases from 50 J to 400 J (a, d, e, f, g), bending lines and discontinuous reactants are formed at the interface of the welding position. And in the 400 J samples (g), the weld gap completely disappeared in the SEM without any traces of voids and cracks, which demonstrates metallurgical bonding. Obvious differences in the oxygen distribution maps between 50 J and 400 J can be found in Fig. 2(c) and (i). The oxygen element is rich in the tiny defects on weld in the 50 J distribution map (Fig. 2(c)), while the oxygen element in the 400 J sample is uniformly distributed in the whole map (Fig. 2(i)). This result demonstrates that the weld seam of the sample has disappeared at the welding energy of 400 J, and no obvious oxide aggregation can be observed at the weld seam in it.

High-resolution CT equipment has been used to detect the presence of large weld gaps and defects inside the welded BMG sample. The six cross-sectional CT images at different cutting positions for each welding sample were shown in Fig. 3. It can be clearly seen that with the continuous increase of the welding energy, the welding gap is also continuously narrowed. The higher the welding energy used, the smaller the welding gap can be found. Until the energy reaches 400 J, the weld seam and original interface completely disappear. This is because even though the surface of the sample is precisely machined, an uneven layer is inevitably present. Therefore, when the energy supplied is insufficient to completely connect the metallic glass blocks, the microscopic contact faces of the samples will preferentially undergo plastic deformation to form a regional metallurgical bond. Then when the energy provided by ultrasonic welding machine is enough, the plastic deformation will spread over the sample contact surface or even out of the contact surface. After the intimate contact of the pure metallic glasses is achieved, a metallurgical bond will be formed, and thus the metallic glasses are completely joined, forming a bulk one.

To investigate to mechanical differences between the as cast and the bonded BMGs, the hardness values of welded sectional surfaces with different welding energies were measured and summarized in Fig. 4(a), which can be used to reflect the welding quality. Here, 30 dots (including welding positions) on a line perpendicular to the weld are selected for surface Vickers hardness

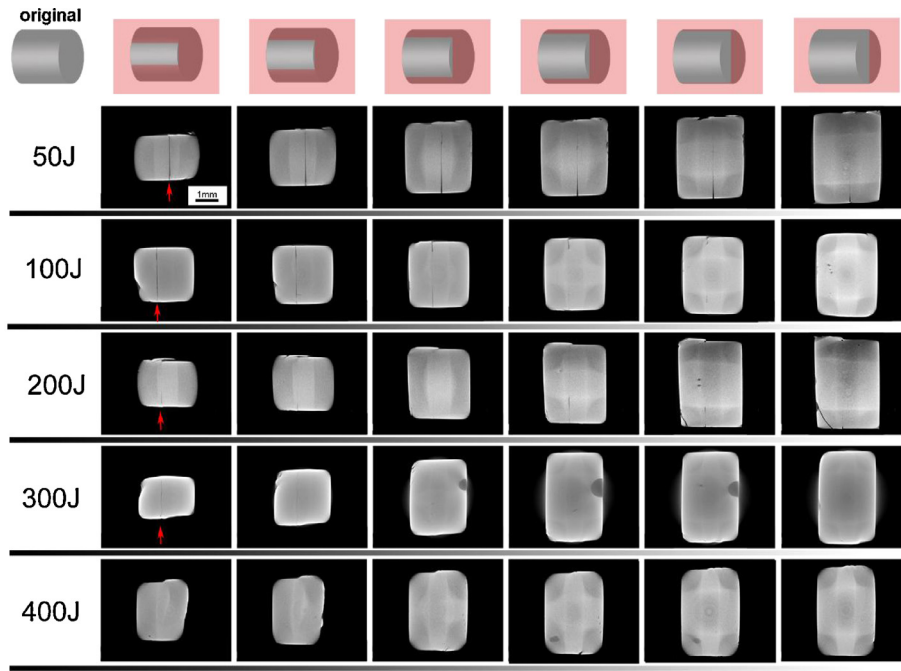


Fig. 3. High resolution CT images of 5 different welding energy samples, and each sample were selected from 6 different positions to show its internal morphology. The picture gradually approaches the center from left to right, and the weld of the 400 J sample on the far right has disappeared.

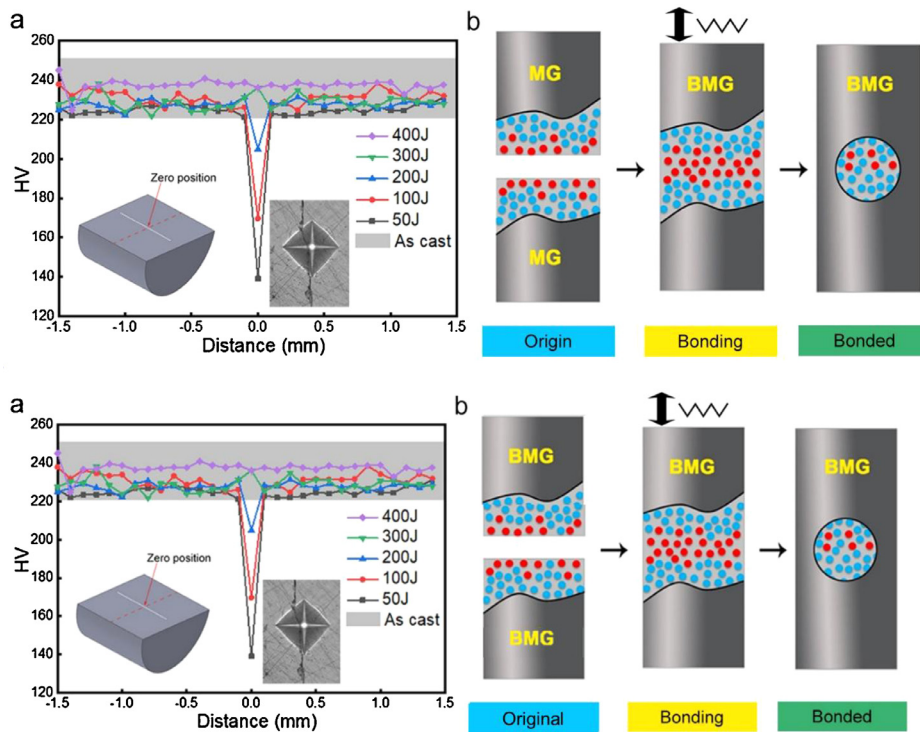


Fig. 4. (a)Micro-hardness test results of 30 dots in the cross section of bonded samples under various energy. Hardness test picture of weld position of the sample with welding energy of 300 J was listed. (b) The cold joining mechanism of metallic glass during the ultrasonic bonding.

testing, and the dot pitches are determined to be 100 μm . From Fig. 4(a), one can see that the average hardness of the samples has a slight increase with the increase of welding energy while the average hardness of the as-cast sample tested is 239.83 (min:220.52, max:251.21). As for the bonded samples with welding energies of 50 J, 100 J and 200 J, there exists a sharp drop of the hardness at the welding interface, indicating that the weld seam is not firm enough and collapses under the hardness testing, as showed

in the illustration. However, when the welding energy went up to 300 J and 400 J, the hardness drop disappeared, exhibiting a flat curve which could be the evidence of the bonding. The results show that the ultrasonic welding between metallic glasses is acceptable when the applied energy is enough. The Vickers indentation testing can be regarded as a test method of minimum welding strength, because the samples do not separate when the indenter is applied to the weld, the lateral force produced by

this process can be regarded as the welding strength test force.

The calculation method is as follows, $\sigma_{\min} = \frac{F_1}{S} = \frac{\frac{1}{2}F \cdot \tan \frac{136^\circ}{2}}{\pi(5 \div 2)^2 \div 2\text{mm}^2} = \frac{\frac{1}{2} \times 4.90\text{N} \div 2.47 = 0.99\text{N}}{\pi(5 \div 2)^2 \div 2\text{mm}^2} = 0.10\text{Mpa}$ where σ_{\min} , F_1 , S , F are minimum welding strength, lateral force, weld area of test sample, indentation load. According to the indentation method [35], the fracture toughness of the bonded sample was calculated to be 4.56 MPa m^{1/2}.

It is widely accepted that amorphous alloys exhibit particular surface mobility behavior compared with the crystals. In conventional wisdom, the disordered materials like metallic glasses were commonly perceived to behave elastic without energy dissipation under low stress loading. However, contrary to this common notion, metallic glasses could behave like dissipative rubbers when subject to a cyclic stress at an ultrasonic frequency. It has been discovered recently that the surface mobility in amorphous materials is much faster than that in bulk from the studies of a variety of glassy solids [36], including glassy polymers [37], oxide glasses [38], organic glasses [39], metallic glasses [40] et al. Strong evidence also demonstrated that such a surface effect can be extended far thick to the nanometer range for amorphous solids, however, only limited to mono atomic layers for crystalline solids [41–42]. In other words, atomic diffusion (or viscosity) on the surface of metallic glass could be millions of times higher (or lower) than that in bulk even at a temperature much lower than the glass transition point [40]. In present work, the cold joining of metallic glasses is closely related with such dynamics and can be illustrated in Fig. 4(b). The surfaces has high atomic mobility, when the ultrasonic vibration starts, the interfaces were adhered with each other owing to the viscous flow of the surface layer.

We have developed a novel method to break through the glass forming ability of BMG. The La₅₅Al₂₅Ni₅Cu₁₀Co₅ metallic glass joints have been successfully fabricated by ultrasonic welding. By adjusting the welding parameters properly, the bonding zone formed by the two samples without any filler has not crystallized, and their thermal properties have hardly changed. With the increase of welding energy, the weld seams in the cross-section of the sample have gradually narrowed to disappear completely, and the hardness of the weld seam has gradually increased to the same level as that of the base metal. Ultrasound bonding technology has been applied to the connection between metallic glass, which will promote the fabrication of bulk amorphous alloys from micro metallic glasses and metallic glasses parts with complex shapes, and even recombine damaged metallic glass parts, so as to widen the narrow application fields of metallic glasses at present.

Declaration of Competing Interest

No conflict of interest exists in the submission of this manuscript, and manuscript is approved by all authors for publication. I would like to declare on behalf of my co-authors that the work described was original research that has not been published previously, and not under consideration for publication elsewhere, in whole or in part. All the authors listed have approved the manuscript that is enclosed.

Acknowledgments

The work was supported by the Key Basic and Applied Research Program of Guangdong Province, China (Grant No. 2019B030302010), the National Key Research and Development Program of China (Grant No. 2018YFA0703605), the National Science Foundation of China (Grant No. 51871157, 51971150), the Science and Technology Innovation Commission Shenzhen (Grants No. JCYJ20170412111216258).

References

- [1] W. Klement, R.H. Willens, P. Duwez, *Nature* 187 (4740) (1960) 869–870.
- [2] B. Lin, X. Bian, P. Wang, G. Luo, *Mater. Sci. Eng., B* 177 (1) (2012) 92–95.
- [3] A. Inoue, A. Takeuchi, *Acta Mater.* 59 (6) (2011) 2243–2267.
- [4] R. Ott, C. Fan, J. Li, T. Hufnagel, *J. Non-Cryst. Solids* 317 (1–2) (2003) 158–163.
- [5] Z. Huang, X. Liang, C. Chang, J. Ma, *Biomed. Microdevices* 21 (1) (2019) 13.
- [6] P. Lowhaphandu, J.J. Lewandowski, *Scr. Mater.* 38 (12) (1998).
- [7] R. Narayan, K. Boopathy, I. Sen, D. Hofmann, U. Ramamurty, *Scr. Mater.* 63 (7) (2010) 768–771.
- [8] M.Z. Ma, R.P. Liu, Y. Xiao, D.C. Lou, L. Liu, Q. Wang, W.K. Wang, *Mater. Sci. Eng., A* 386 (1–2) (2004) 326–330.
- [9] A. Inoue, *Acta Mater.* 48 (1) (2000) 279–306.
- [10] M.M. Khan, I. Shabib, W. Haider, *Scr. Mater.* 162 (2019) 223–229.
- [11] J.Q. Wang, Y.H. Liu, M.W. Chen, G.Q. Xie, D.V. Louzguine-Luzgin, A. Inoue, J.H. Perepezko, *Adv. Funct. Mater.* 22 (12) (2012) 2567–2570.
- [12] J. Wang, R. Li, N. Hua, L. Huang, T. Zhang, *Scr. Mater.* 65 (6) (2011) 536–539.
- [13] M. Katter, J. Wecker, L. Schultz, *J. Appl. Phys.* 70 (6) (1991) 3188–3196.
- [14] J. Ma, X. Liang, X. Wu, Z. Liu, F. Gong, *Sci Rep* 5 (1) (2015) 1–6.
- [15] M. Ashby, A. Greer, *Scr. Mater.* 54 (3) (2006) 321–326.
- [16] A.L. Greer, *Science* 267 (5206) (1995) 1947–1953.
- [17] Q. Zhang, H. Zhang, Y. Deng, B. Ding, Z. Hu, *Scr. Mater.* 49 (4) (2003) 273–278.
- [18] M. Jiang, B. Huang, Z. Jiang, C. Lu, L. Dai, *Scr. Mater.* 97 (2015) 17–20.
- [19] L. Shao, A. Datsy, J. Huang, J. Ketkaew, J. Schroers, *Sci. Rep.* 7 (1) (2017) 7989.
- [20] J. Kim, Y. Kawamura, *Scr. Mater.* 56 (8) (2007) 709–712.
- [21] Y. Kawamura, Y. Ohno, *Scr. Mater.* 45 (2) (2001) 127–132.
- [22] S. Fukumoto, A. Soeda, Y. Yokoyama, M. Minami, M. Matsushima, K. Fujimoto, *Sci. Technol. Weld. Join.* 18 (2) (2013) 135–142.
- [23] J.C. Trenkle, T.P. Weihs, T.C. Hufnagel, *Scr. Mater.* 58 (4) (2008) 315–318.
- [24] Y. Kawamura, *Mater. Sci. Eng., A* 375 (1) (2004) 112–119.
- [25] M. Maeda, Y. Takahashi, M. Fukuhara, X.M. Wang, A. Inoue, *Mater. Sci. Eng., A* 148 (1–3) (2008) 141–144.
- [26] J. Ma, C. Yang, X. Liu, B. Shang, Q. He, F. Li, T. Wang, D. Wei, X. Liang, X. Wu, *Sci. Adv.* 5 (11) (2019) eaax7256.
- [27] Y. Kawamura, Y. Ohno, *Scr. Mater.* 45 (3) (2001) 279–285.
- [28] X. Zhang, Y. Xiao, L. Wang, C. Wan, Q. Wang, H. Sheng, M. Li, *Ultrason. Sonochem.* 45 (2018) 86–94.
- [29] A. Siddiq, E. Ghassemieh, *Int. J. Adv. Manuf. Technol.* 54 (9–12) (2011) 997–1009.
- [30] S. Kumar, C.S. Wu, G.K. Padhy, W. Ding, *J. Manuf. Processes* 26 (2017) 295–322.
- [31] W. Wu, J. Jiang, G. Li, J.Y.H. Fuh, H. Jiang, P. Gou, L. Zhang, W. Liu, J. Zhao, *J. Non-Cryst. Solids* 506 (2019) 1–5.
- [32] J. Kim, *Mater. Lett.* 130 (2014) 160–163.
- [33] X. Zhang, Y. Xiao, L. Wang, C. Wan, Q. Wang, H. Sheng, M. Li, *Ultrason. Sonochem.* 45 (2018) 86–94.
- [34] L.C. Chen, F. Spaepen, *J. Appl. Phys.* 69 (1991) 679.
- [35] D.S. Harding, W.C. Oliver, G.M. Pharr, *Mater. Res. Soc. Symp. Proc.* 356 (1995) 665.
- [36] J.D. Stevenson, P.G. Wolynes, *J. Chem. Phys.* 129 (23) (2008) 234514.
- [37] Z. Fakhraai, J.A. Forrest, *Science* 319 (5863) (2008) 600–604.
- [38] L. Wang, A.J.G. Ellison, D.G. Ast, *J. Appl. Phys.* 101 (2) (2007) 77–43.
- [39] L. Zhu, C.W. Brian, S.F. Swallen, P.T. Straus, M.D. Ediger, L. Yu, *Phys. Rev. Lett.* 106 (25) (2011) 256103.
- [40] C.R. Cao, Y.M. Lu, H.Y. Bai, W.H. Wang, *Appl. Phys. Lett.* 107 (14) (2015) 577.
- [41] Y. Chai, T. Salez, J.D. McGraw, M. Benzaquen, K. Dalnoki-Veress, E. Raphaël, J.A. Forrest, *Science* 343 (6174) (2014) 994.
- [42] F. Chen, C.H. Lam, O.K.C. Tsui, *Science* 343 (6174) (2014) 975–976.